International Conference on Applied Energy 2019
Aug 12-15, 2019, Västerås, Sweden
Paper ID: 123

DESIGN AND OPTIMAZATION OF THE COMPOUND PARABOLIC CONCENTRATORS (CPCS) WITH VARIOUS TRUNCATION POSITIONS

Gaoming Zhang[1], Jinjia Wei [1, 2*]

1 State Key Laboratory of Multiphase Flow in Power Engineering, Xi'an Jiaotong University, Xi'an, Shaanxi 710049, China

2 School of Chemical Engineering and Technology, Xi'an Jiaotong University, Xi'an, Shaanxi 710049, China (Corresponding Author)

ABSTRACT

In our previous work, a traditional compound parabolic concentrator (CPC) was truncated from the positions where multiple reflections exist and a novel CPC with high efficiency and uniform flux was obtained and defined as EMR concentrator. We also figured out that there existed the highest and lowest truncation positions in EMR concentrators, which were defined as HEMR and LEMR concentrators respectively. In the present work, our objective is to design EMR concentrators with various truncation positions and obtain the optimal truncation position. Firstly, based on the geometry topology, EMR concentrators with various truncation positions were designed. Ray tracing simulation of EMR concentrators was conducted by TracePro to figure out their optical efficiencies and irradiance non-uniformities. Results showed optical efficiencies of EMR concentrators with various truncation positions were almost the same, but irradiance uniformities exhibited some difference. On one hand, for EMR concentrators with truncation positions between HEMR and LEMR, irradiance non-uniformity increases slightly with a drop in truncation position firstly and then decreases slightly. On the other hand, for EMR concentrators further truncated than LEMR, irradiance uniformity increases rapidly with a drop in truncation position. Thus, LEMR concentrator is likely to be the EMR concentrator with the optimal truncation position due to its best tradeoff between optical performance and material consumption.

Keywords: Compound parabolic concentrator; Eliminating multiple reflections; Optical efficiency; Non-uniform irradiance; Optimal truncation position;

NONMENCLATURE

Abbreviations	
EMR	eliminating multiple reflections
Symbols	
$\overline{BF}$	width of outlet aperture (mm)
C	concentration ratio
f	focal length of the parabola (mm)
G	solar radiation intensity ($W \cdot m^{-2}$)
H	height of concentrator (mm)
ϑ	half acceptance angle (°)
σ	non-uniformity

1. INTRODUCTION

The concentrating photovoltaic and thermal (CPV/T) system, a promising alternative energy source, has been widely investigated recently [1-3]. The adoption of concentrators increases solar flux on solar cells and improves the electrical and thermal output of CPV/T systems. Among all kinds of concentrators, the compound parabolic concentrator (CPC) is widely applied in CPV/T systems due to its large acceptance angle, ability to harvest solar diffuse radiation and high optical efficiency [4-6]. In general, the full CPC is two high and truncation is always adopted to reduce the height and improve uniformity as well. In our previous study [7], a novel truncation method of eliminating multiple reflections within CPC was proposed and the truncated CPC eliminating multiple reflections was defined as EMR concentrator. In fact, there existed the highest and lowest truncation positions in EMR concentrators, which were what we called HEMR and LEMR respectively [8]. However, EMR concentrators with truncation positions

Selection and peer-review under responsibility of the scientific committee of the 11th Int. Conf. on Applied Energy (ICAE2019).

between HEMR and LEMR and lower than LEMR have never been studied yet.

In the present study, our objective is to investigate the effect of truncation position of EMR concentrator on its optical performance and figure out the optimal truncation position of EMR concentrators. Firstly, based on the geometry topology, equation group was established to design EMR concentrators with various truncation positions. Besides, ray tracing of EMR concentrators with various truncation positions was conducted by TracePro. The optical efficiencies and irradiance non-uniformities of EMR concentrators were analyzed with various truncation positions.

2. DESIGN OF EMR CONCENTRATORS WITH VARIOUS TRUNCATION POSITIONS

2.1 Principle of EMR design

The concentrators are designed based on the principle of EMR, which was described in detail in our previous work [7, 8], and equation groups for designing HEMR and LEMR concentrators are shown as follows respectively:

$$\begin{cases} 16\left(\sin^2\theta+\sin\theta\right)t_C{}^4+8\left(3\sin^2\theta+\sin\theta-1\right)t_C{}^2+(-16\sin\theta\cos\theta)t_C+(-3\sin^2\theta+\sin\theta+2)=0 \\ 4\overline{BF}\left(\sin\theta\cos\theta+\cos\theta\right)t_C{}^2+4\overline{BF}\left(\sin^2\theta+\sin\theta\right)t_C-\left(\overline{BF}\sin\theta\cos\theta+\overline{BF}\cos\theta+2H\right)=0 \\ 4\left(\sin^2\theta+\sin\theta\right)t_C{}^2-4\left(\sin\theta\cos\theta+\cos\theta\right)t_C-\left(\sin^2\theta+\sin\theta-C_{EMR}-1\right)=0 \\ \overline{BF}\left(\sin\theta+1\right)-2f=0 \end{cases} \tag{1}$$

$$\begin{cases} 16\left(\sin^2\theta+\sin\theta\right)t_C{}^4+\left(32\sin^2\theta+8\sin\theta-4\right)t_C{}^2+8\sin\theta\cos\theta\left(\tan^2\theta-2\right)t_C+(-5\sin^2\theta+\sin\theta+1)=0 \\ 4\overline{BF}\left(\sin\theta\cos\theta+\cos\theta\right)t_C{}^2+4\overline{BF}\left(\sin^2\theta+\sin\theta\right)t_C-\left(\overline{BF}\sin\theta\cos\theta+\overline{BF}\cos\theta+2H\right)=0 \\ 4\left(\sin^2\theta+\sin\theta\right)t_C{}^2-4\left(\sin\theta\cos\theta+\cos\theta\right)t_C-\left(\sin^2\theta+\sin\theta-C_{EMR}-1\right)=0 \\ \overline{BF}\left(\sin\theta+1\right)-2f=0 \end{cases} \tag{2}$$

In equation groups (1) and (2), there are four equations and six unknown variables: the half acceptance angle ϑ, the parameter of top point (point *C*) of the parabola t_C, the width of outlet aperture $\overline{BF}$, the height of the concentrator *H*, the concentration ratio of the concentrator C_{EMR} and the focal length of the parabola *f*. In general, the width of the outlet aperture $\overline{BF}$ and the concentration ratio of the concentrator C_{EMR} are given, so these two equation groups can be solved. The difference between these two equation groups is just the first equation of each equation group. The reason falls into the difference between the reflected lines of the incident lights parallel to the axis of CPC in the cases of HEMR and LEMR designs. As shown in Fig. 1, for HEMR design, C_hA_h is the reflected lines of the incident light M_hC_h and goes through the bottom point of the parabola C_hB_h. But for LEMR design, as the reflected lines of the incident light M_lC_l, C_lA_l will hit the midpoint (A_l) of the best concentration plane $B_{l1}F_{l1}$.

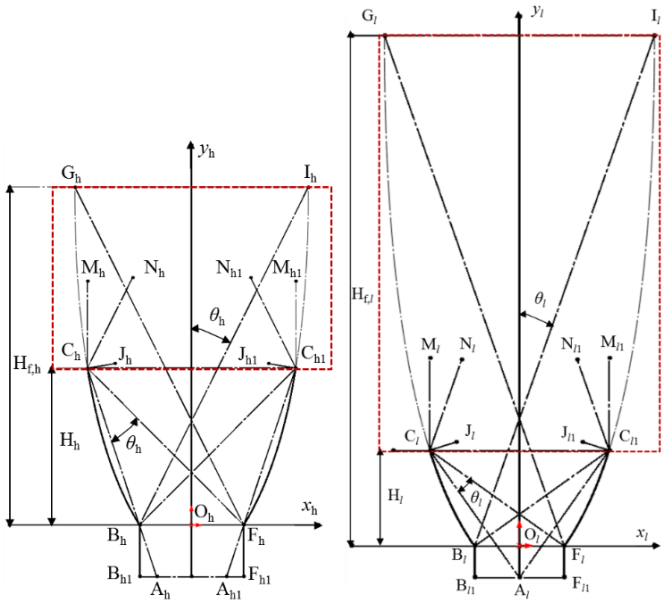

Fig. 1 Schematic of the design for HEMR (left) and LEMR (right) concentrators

2.2 EMR concentrators with various truncation positions

As shown in Fig. 2, it can be inferred that for EMR concentrators with truncation positions between HEMR and LEMR, the reflected line (*CA*) of the incident light (*MC*) parallel to the axis of CPC will hit a point between A_h and A_l. And for EMR concentrators with truncation positions lower than LEMR, the reflected lines of the incident light parallel to the axis of CPC will hit a point between A_l and F_1. For EMR with any truncation position, we assume the reflected lines (*CA*) of the incident light (*MC*) meets the outlet aperture *BF* at point *Q* and the line *CP* is perpendicular to the line *BF* at point *P*. Because *CQ* is the

reflected line of *MC* and *CF* is the reflected line of incident light *NC* which is parallel to the axis of the parabola *CB*, $\angle QCF$ is equal to $\angle MCN$, which is the half acceptance angle of CPC ϑ. According to the triangle relationship, $\angle CQP$ is equal to the sum of $\angle QCF$ and $\angle CFQ$. Thus tan $\angle CQP$ can be calculated by:

$$\tan\angle \mathrm{CQP} = \frac{\tan\theta + \tan\angle \mathrm{CFQ}}{1 - \tan\theta \tan\angle \mathrm{CFQ}} \tag{3}$$

where tan $\angle CFQ$ can be given by:

$$\tan\angle \mathrm{CFQ} = \frac{\overline{CP}}{\overline{PF}} = \frac{H}{\overline{BF}/2 - x_C} \tag{4}$$

where x_C is *x*-coordinate of the top point (point C) of the parabola *CB*, which can be obtained from the concentration ratio C_{EMR} and the width of the outlet aperture $\overline{BF}$:

$$x_C = -C_{EMR} \cdot \overline{BF}/2 \tag{5}$$

Substituting equations (4) and (5) into equation (3) can obtain:

$$\tan\angle \mathrm{CQP} = \frac{\tan\theta + 2H/\left[\left(1+C_{EMR}\right)\overline{BF}\right]}{1 - 2H\tan\theta/\left[\left(1+C_{EMR}\right)\overline{BF}\right]} \tag{6}$$

By replacing the first equation in equation group (1) or (2) with equation (6), the equation group for designing EMR concentrators with various truncation positions can be obtained:

$$\begin{cases} \tan\angle \mathrm{CQP} = \dfrac{\tan\theta + 2H/\left[\left(1+C_{EMR}\right)\overline{BF}\right]}{1 - 2H\tan\theta/\left[\left(1+C_{EMR}\right)\overline{BF}\right]} \\ 4\overline{BF}\left(\sin\theta\cos\theta + \cos\theta\right)t_C{}^2 + 4\overline{BF}\left(\sin^2\theta + \sin\theta\right)t_C - \left(\overline{BF}\sin\theta\cos\theta + \overline{BF}\cos\theta + 2H\right) = 0 \\ 4\left(\sin^2\theta + \sin\theta\right)t_C{}^2 - 4\left(\sin\theta\cos\theta + \cos\theta\right)t_C - \left(\sin^2\theta + \sin\theta - C_{EMR} - 1\right) = 0 \\ \overline{BF}\left(\sin\theta + 1\right) - 2f = 0 \end{cases} \tag{7}$$

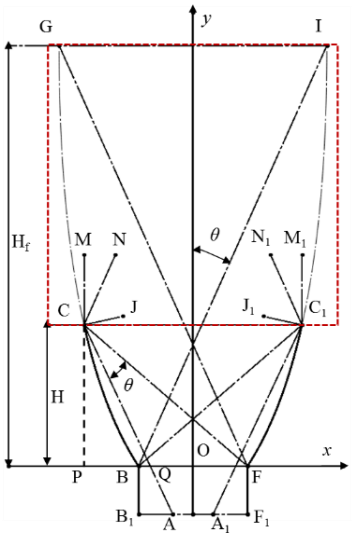

Fig. 2 Schematic of the design for EMR concentrators with any truncation positions

In equation group (7), there are four equations and seven unknown variables: ϑ, *H*, $\overline{BF}$, t_C, *f*, C_{EMR} and $\angle CQP$. Compared with equation group (1) or (2), $\angle CQP$ is an additional variable. To a certain degree, $\angle CQP$ represents the truncation position of EMR concentrator. Larger values of $\angle CQP$ mean higher truncation positions, and vice versa. Under the condition of constant width of outlet aperture, height of concentrator indicates truncation position of EMR concentrator as well.

3. RAY TRACING OF EMR CONCENTRATORS

Fig. 3 shows schematic of rays tracing simulation of EMR concentrators in TracePro. It can be seen that reflecting surfaces of the concentrator are defined as reflectors with reflectivity of 0.94. Upper surface of the receiver is defined as a perfect absorber with 100% absorptivity. Then two rectangular sources are defined over the inlet aperture of the concentrator. One is defined as direct normal irradiance source (marked as DNI) and the other one is defined as diffuse source (marked as DIF). For both sources, grid pattern is random and 2.5 million rays are emitted and uniformly distributed. For DNI source, irradiance is set to be 765W/m^2 and direction of rays is parallel to the axis of the concentrator (y axis). For DIF source, irradiance is set to be 135W/m^2 and direction of rays varies from 0° to 90° with respect to the axis of the concentrator.

Once the sources, the reflectors and the absorber are defined, rays tracing simulation can be conducted to obtain optical performances of EMR concentrators, which include optical efficiency and irradiance non-uniformity. For optical efficiency, it can be calculated by the ratio of the energy received by the absorber to the energy received by the inlet aperture of the concentrator:

$$\eta_{EMR} = \frac{\overline{G}_{abs} \cdot A_{abs}}{G_t \cdot A_{in}} = \frac{\overline{G}_{abs}}{G_t \cdot C_{EMR}} \tag{12}$$

where $\overline{G}_{abs}$ is the average irradiance received by the absorber, A_{abs} is the collecting area of the absorber, G_t is the total solar irradiance at the inlet aperture of the concentrator and A_{in} is the area of the inlet aperture. For irradiance non-uniformity, it can be characterized by standard deviation of the irradiance illuminating on the absorber:

$$\sigma_G = \frac{1}{G_{ref}} \sqrt{\frac{1}{n} \sum_{i=1}^{n} \left[G_{abs}(i,j) - \overline{G}_{abs} \right]^2} \tag{13}$$

where σ_G is a dimensionless standard deviation non-uniform factor, G_{ref} is the solar irradiance under reference conditions (1000W/m^2) and is used to make the standard deviation non-uniform factor dimensionless, n is the number of discrete elements along the width direction of the absorber, G_{abs} (i, j) is the average irradiance illuminating on the absorber element (i, j) and i and j are the absorber element labels along the width and length directions.

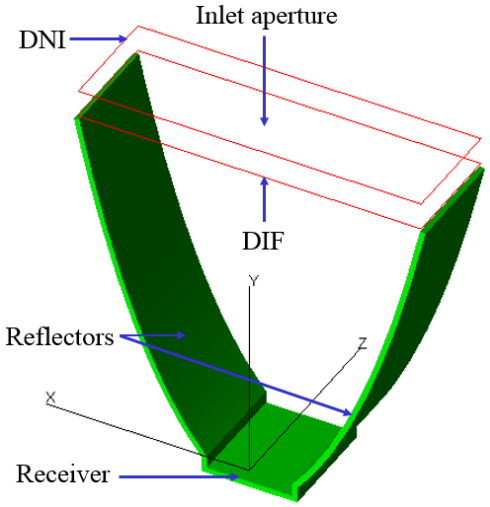

Fig. 3 Schematic of rays tracing simulation in TracePro

4. RESULTS AND DISCUSSION

4.1 Optical efficiencies of EMR concentrators

As shown in Fig. 4, with a decrease in $\angle CQP$, the height of EMR concentrator experiences a decrease as well. However, optical efficiencies of EMR concentrators with various truncation positions are almost the same, which means that truncation position has little effect on the optical efficiency of EMR concentrator.

4.2 Irradiance distribution of EMR concentrators

From Figs. 5 and 6, irradiance distribution profiles of EMR concentrators with different truncation positions exhibit obvious difference. Fig. 5 illustrates irradiance distribution profiles of EMR concentrators with height from 568mm to 703mm. It can be seen that the irradiance in the central region of the absorber is quite uniform in the case of 703mm height (HEMR case). When the height of EMR concentrator decreases from 703mm to 568mm, the width of this irradiance uniform region decreases and the irradiance in the central region of the absorber increases. Interestingly, the irradiance non-uniformity doesn't increase monotonically with decreasing concentrator height. From Fig. 7, irradiance non-uniformity increases slightly from 0.652 to 0.808 firstly and then decreases slightly from 0.808 to 0.691 when concentrator height decreases from 703mm to 568mm. Irradiance non-uniformity reaches its local maximum of 0.808 at the height of 656mm.

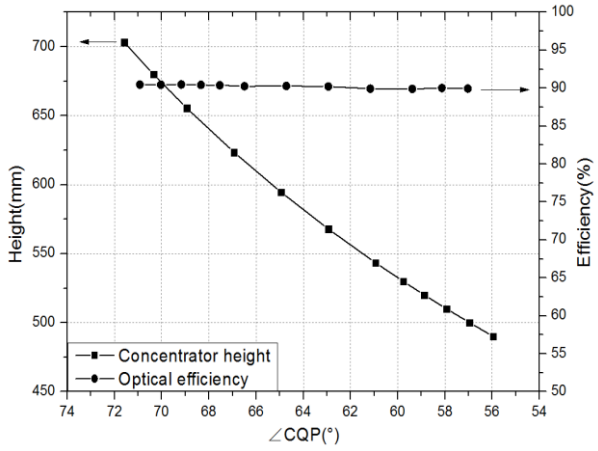

Fig. 4 Variations in concentrator height and optical efficiency

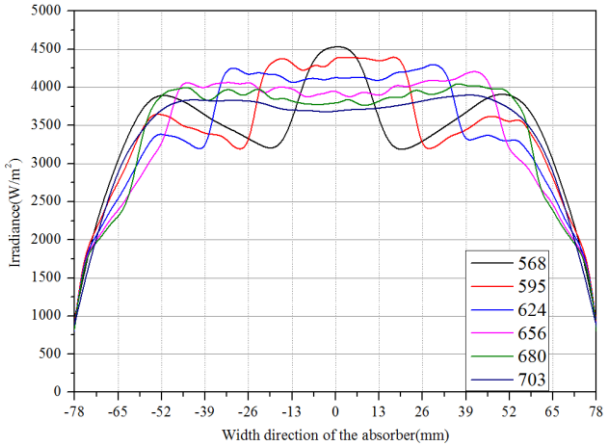

Fig. 5 Irradiance profiles of EMR (concentrator height from 568mm to 703mm)

As shown in Fig. 6, when concentrator height decreases further and is less than 543mm (LEMR case), the irradiance in the central region of the absorber decreases a lot due to absence of EMR concentration. And the width of this low irradiance region increases with decreasing concentrator height. Besides, with a decrease in concentrator height, two symmetric peaks of irradiance profiles become more and more pronounced and shift to the edge of the width of the absorber. Both the increasing

width of the low irradiance region and gradually pronounced peaks indicate increasing irradiance non-uniformity, which is in good agreement with what Fig. 7 exhibits. From Fig. 7, irradiance non-uniformity increases monotonically from 0.678 to 2.0 when concentrator height decreases from 543mm to 490mm.

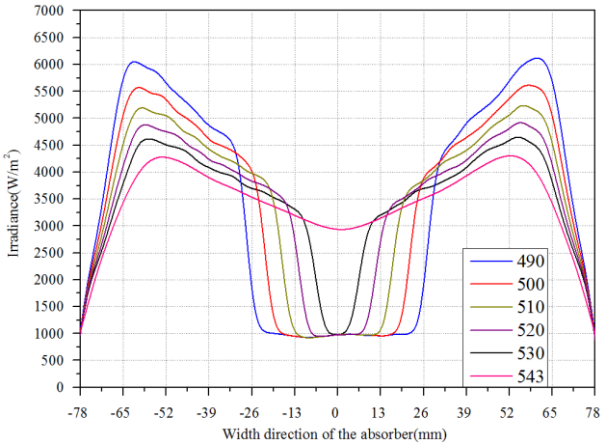

Fig. 6 Irradiance profiles of EMR (concentrator height from 490mm to 543mm)

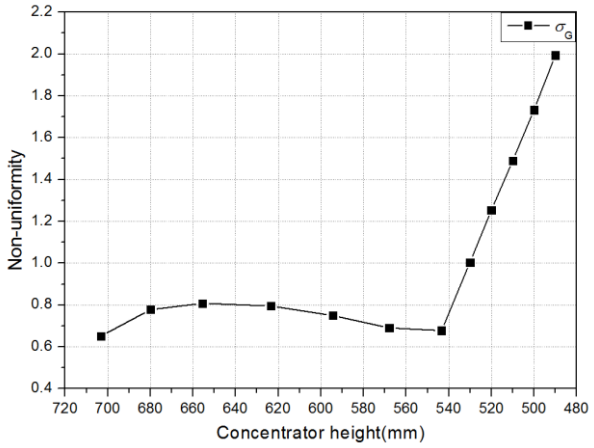

Fig. 7 Irradiance non-uniformity of EMR (concentrator height from 490mm to 703mm)

5. CONCLUSIONS

In the present study, we proposed a method to design EMR concentrators with various truncation positions. Ray tracing of EMR concentrators was conducted by TracePro. The optical efficiencies and irradiance non-uniformities of EMR concentrators were analyzed. Results showed that HEMR and LEMR are the best alternatives among EMR concentrators with various truncation positions. Meanwhile, height of LEMR is just 77% of that of HEMR, which means not only less material consumption and lower manufacturing cost but also facilitating installation, operation and maintenance of the CPV/T system. Thus LEMR is likely to be the EMR concentrator with optimal truncation position. Furthermore, future work will be carried out on electrical and thermal performances of CPV/T systems to verify this point.

ACKNOWLEDGEMENTS

The present work is supported by Yulin Science and Technology Project (NO.2017KJJH-03), the Key Research Project of Shaanxi Province (No.2017ZDXM-GY-017), the Fundamental Research Funds for the Central Universities (No.cxtd2017004), Innovation Capacity Support Program of Shaanxi Province (No.2019TD-039) and Project supported by the Funds of International Cooperation and Exchange of the National Natural Science Foundation of China (No. 51961135102).

REFERENCES

[1] Feng C, Zheng H, Wang R, et al. Performance investigation of a concentrating photovoltaic/thermal system with transmissive Fresnel solar concentrator [J]. Energy Conversion and Management, 2016, 111:401-408

[2] Yazdanifard F, Ebrahimnia-Bajestan E, Ameri M. Performance of a parabolic trough concentrating photovoltaic/thermal system: Effects of flow regime, design parameters, and using nanofluids [J]. Energy Conversion & Management, 2017, 148:1265-1277.

[3] Youssef WB, Maatallah Taher, Menezo Christophe, et al. Modeling and optimization of a solar system based on concentrating photovoltaic/thermal collector [J]. Solar Energy, 2018, 170:301-313

[4] Abdelhamid M, Widyolar B K, Jiang L, et al. Novel double-stage high-concentrated solar hybrid photovoltaic/thermal (PV/T) collector with nonimaging optics and GaAs solar cells reflector[J]. Applied Energy, 2016, 182:68-79.

[5] Atheaya D, Tiwari A, Tiwari G N, et al. Performance evaluation of inverted absorber photovoltaic thermal compound parabolic concentrator (PVT-CPC): Constant flow rate mode [J]. Applied Energy, 2016, 167:70-79.

[6] Zhang G, Wei J, Xie H, et al. Performance investigation on a novel spectral splitting concentrating photovoltaic/thermal system based on direct absorption collection [J]. Solar Energy, 2018, 163:552-563

[7] Xie H, Wei J, Wang Z, et al. Design and performance research on eliminating multiple reflections of solar radiation within compound parabolic concentrator (CPC) in hybrid CPV/T system [J]. Solar Energy, 2016, 129:126-146.

[8] Xie H, Wei J, Wang Z, et al. Design and performance study of truncated CPC by eliminating multiple reflections of solar radiation in hybrid CPV/T system: Highest and lowest truncation position [J]. Solar Energy, 2016, 136:217-225.